Urban Resilience and Sustainability

Urban Resilience Sustainability, 3(1): 57–85.
DOI: 10.3934/urs.2025003
Received: 28 March 2025
Revised: 22 May 2025
Accepted: 4 June 2025
Published: 11 June 2025

https://www.aimspress.com/journal/urs

Research article

An assessment framework for evaluating urban flood vulnerabilities using Night-Time Light data

Nuwani Kangana[1] and Nayomi Kankanamge[2,*]

[1] Department of Town and Country Planning, University of Moratuwa, Sri Lanka
[2] School of Law and Society, University of the Sunshine Coast, Moreton Bay, QLD 4502, Australia

*** Correspondence:** Email: nkankanamge@usc.edu.au; Tel: +61754563059.

Abstract: Urban floods pose significant socio-economic and environmental challenges, particularly in rapidly urbanizing regions. We utilized Night-Time Light (NTL) data as a dynamic proxy for human activity and urban density to enhance the assessment of urban flood vulnerability. Unlike traditional methods that rely on static datasets or post-disaster surveys, this approach incorporates real-time NTL data to better capture the evolving patterns of urban exposure. Focusing on the Kelani River watershed, the most flood-prone and densely populated region in Sri Lanka, we integrated nine conditioning factors, including slope, precipitation, and soil type, with NTL intensity to generate comprehensive vulnerability maps. To ensure the accessibility and practical application of the results, a web application was developed using Google Earth Engine (GEE), offering an interactive platform for real-time visualization of urban flood risks. The findings underlined the transformative potential of NTL data in flood vulnerability mapping and demonstrated its applicability as a cost-effective, scalable, and open-access decision-support tool adaptable to various urban contexts.

Keywords: Night-Time Light data; urban flooding; urban resilience; vulnerability assessment; web application

1. Introduction

Urban flooding is the inundation of an urbanized area with water, typically occurring due to high precipitation on impervious surfaces [1]. As noted in recent research, urban floods cause severe socio-economic impacts, resulting in substantial damage to urban infrastructure, property, and the

environment. In fact, urban flooding is the most frequent natural disaster, accounting for 44% of total disaster events from 2000 to 2019, with 2 billion people globally at risk [2].

A key approach in assessing the impacts of natural disasters like urban flooding is vulnerability mapping, which is considered more crucial than hazard mapping. As depicted in Figure 1, hazard mapping typically focuses on the probability of flood occurrence based on parameters such as magnitude and frequency, while vulnerability mapping evaluates the exposure of human assets, such as people, infrastructure, housing, and production capacities, to flood risks [3–5]. This distinction is emphasized in contemporary studies, such as those by Agonafir et al., [6] who highlighted the increasing role of advanced urban flood modeling techniques, including machine learning and crowdsourced data to improve flood risk assessments.

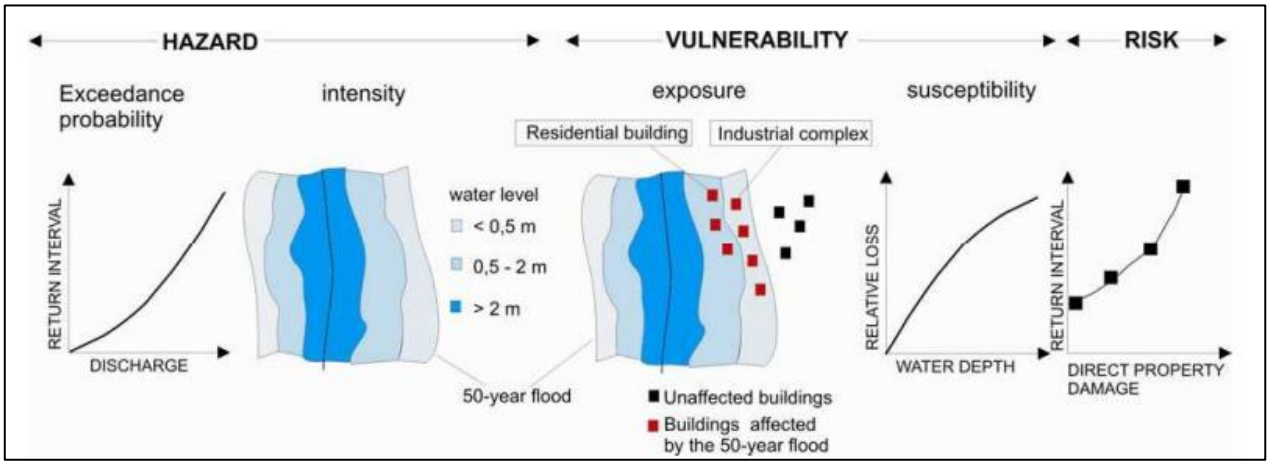

Figure 1. Difference between disaster hazard, vulnerability, and risk.

Given the rapid urbanization and the increasing frequency of climate change-induced extreme weather, comprehensive flood research is more critical than ever. Urban areas, with their impervious surfaces, are particularly vulnerable to flooding. As people concentrate in flood-prone cities, the impact of urban flooding intensifies. Researchers are focusing on data-driven modeling techniques to improve flood prediction, response, and mitigation strategies, especially as climate change is expected to increase storm intensity and strain urban infrastructure [6].

Different qualitative and quantitative approaches were used in previous studies to map out the human flood exposure levels to urban flooding. Most qualitative approaches utilized data from interviews and questionnaire surveys for socio-economic analyses. High-resolution population data and land use data were the most used data sources for quantitative analyses to understand the gravity of flood exposure levels [5,7,8].

Such contemporary approaches in assessing human exposure to urban floods are for post-flood impact assessments. For instance, interviews and questionnaire surveys about the affected communities are often carried out a few weeks or months after a flood event. On the other hand, the quantitative approach, which considers population density and land use changes, have the limitation of sparse data availability on land use changes in developing countries, including Sri Lanka [4,9]. Further, the population density represents the residential activities but does not accurately represent urbanized hotspots, which are important to examine during an urban flood. Accordingly, such methods'

inability to trace the rapid changes in an urban setting, which is a key determinant in urban flood vulnerability assessment, can be identified as the main limitation [7,8].

Therefore, we attempt to use Night-time Light Data (NTL) as a novel source of data to expedite the vulnerability assessment process. It is an open data source that anyone can access with no cost. VIIRS, which is the latest NTL observation satellite, has been identified as an economic and population indicator, which specifies the urbanized areas [10,11]. NTL delivers spatially clear observations from synthetic lighting through human settlements at night [12]. We, therefore, aim to integrate NTL data into vulnerability mapping to provide a more dynamic and real-time assessment of urban flood risks, bypassing the constraints of traditional methods. Against this backdrop, the main research questions of this study include: (a) How to assess urban flood vulnerability levels using NTL Data? and (b) How to develop a user-friendly web application to visualize the urban flood vulnerability levels?

2. Literature review

2.1. Urban floods

Urban flood refers to a temporary inundation of an urbanized area with water that is usually dry [1]. This is commonly called a "Localized Flood" or "Drainage Congestion". This may occur due to the overflowing of a waterbody or inundation of an area with stormwater collected with high precipitation and low infiltration [13]. The magnitude of urban floods varies with the depth, extent, and duration of the flood inundation area. Urban flooding is growing each year, specifically in South Asian countries [14]. This is due to several factors, including severe weather changes, overwhelming stormwater drainage capacity, land use alterations, and man-made changes to the soil structure due to rapid urbanization [15].

Urban floods rarely result in loss of lives, while the disturbance to day-to-day urban activities, loss of property, damage to infrastructure networks, disruption of economic activities, and spread of diseases are highly influential impacts [16], which disturbs the urban livelihood. As cities act as the economic engines of a country, urban flood-induced negative impacts could create massive losses directly to the city economy and indirectly to the entire nation. Therefore, it is important to assess the changing urban flood vulnerability in urban areas to enhance the preparedness of the cities [17].

2.2. Urban flood vulnerability mapping

Urban flood vulnerability refers to a situation in which the people, properties, economy, infrastructure, housing, production capacities, and other tangible human assets in flood-prone areas being a victim of flooding. On the other hand, the ecological system gets exposed to the negative consequences of flood occurrence [18]. The first vulnerability study related to urban flooding was done in the USA and Great Britain around the 1970s. Since then, most of the vulnerability studies related to urban flooding were conducted with a focus on socioeconomic analyses conducted during the post-flood situation [7].

Urban flood vulnerability is defined by different authors in different ways. For instance, the researchers in [19] discussed different aspects of vulnerability, such as social vulnerability, economic vulnerability, urban vulnerability, infrastructure vulnerability, and ecological and environmental vulnerability. However, urban flood vulnerability mapping aims to determine the spatial distribution

of highly concentrated urban activities in flood-risk areas. For that, human exposure to urban floods and flood susceptibility levels needs to be identified in a considered watershed.

Recent advancements in remote sensing and cloud-based geospatial platforms have significantly improved flood vulnerability assessments. Studies such as Sy et al. [20] and Shinde et al. [21] demonstrated the application of Sentinel-1 SAR imagery within Google Earth Engine (GEE) to assess flood inundation extents and quantify urban exposure in real-time. Similarly, Gemitzi et al. [22] and Prasertsoong and Puttanapong [23] developed constantly updated flood risk mapping frameworks using high-resolution land cover and socio-economic indicators integrated within GEE, emphasizing the growing importance of satellite-based automation for flood modeling.

Urban flood vulnerability also depends on the probability of flood occurrence and the situation of the people and other tangible assets exposed to urban floods. This transforms flood hazard into a risk that can cause humans to lose their lives and properties. According to the Asian Disaster Risk Centre [24], urban floods account for 41% of the total disasters in Asian Countries, and it has been the highest influencing disaster, which affects human lives and property. Although flooding is a natural part of the hydrological cycle, rapid urbanization and climatic change have caused an increase in the risk of flooding, specifically converting urban flooding into a topic that needs to be explored further [25].

2.3. Urban flood susceptibility mapping

Flood susceptibility identifies the flood-vulnerable areas based on the physical conditions, topographic features, and other external conditioning factors such as weather, soil types, soil moisture, and infiltration capacity, according to the land cover. Therefore, the susceptibility analysis can be used as the key step towards the vulnerability assessment of urban flooding [26].

To determine urban flood susceptibility and the natural tendency of a flood event to happen, flood modeling has been used so far [27]. According to previous studies, there are three types of flood modeling. These include: (a) Hydrological methods; (b) Statistical methods; and (c) Knowledge-based methods [27,28]. Among them, the Statistical and Knowledge-based methods are the most frequently used methods with higher accuracy and data availability. Also, they have the possibility of incorporating many variables such as topographic features, climatic changes, and land use changes. Traditionally, flood estimation and management have been the domains of hydrologists, water resources engineers, and statisticians, and disciplinary approaches abound. Therefore, for this study, the flood susceptibility analysis has followed Statistical and knowledge-based methods.

2.4. Contemporary tools and techniques used to identify human exposure levels to urban floods

Contemporary approaches used to identify human exposure levels to urban floods can be categorized into three approaches. These include the (a) Qualitative approach; (b) Indicator-based approach; and (c) Quantitative analytical approach. The first vulnerability analysis was based on a decision model that defines how people understand the hazard, a qualitative approach, by Kates in 1971 [29]. Then, it was developed into a multi-disciplinary analysis by Birkmann in 2006 [30] by including physical, economic, and social aspects. However, these studies were based on a qualitative approach, which focuses on people's perceptions.

Thereafter, flood vulnerability analysis was directed towards an indicator-based approach, developing a Flood Vulnerability Index by Balica et al. in 2012 [31]. During 2018–2020, Synthetic

Aperture Radar, Sentinel, 1 and 2 were used in mapping the flood inundation and utilized in deriving the vulnerability of flooding with field surveys. Still, they have forgotten the community aspect of vulnerability mapping. Blistanova et al. [32] developed the multi-criteria analysis using GIS, which includes conditioning factors, and geomorphological features such as slope and soil type. The increasing urbanization and changing climatic patterns were also taken into consideration in the Danish Integrated Assessment System (DIAS) [19,33].

All the aforesaid approaches were used to identify the flood hazard aspect of flood vulnerability, but the human exposure to the flood vulnerability aspect was paid less attention in previous studies [34,35]. Focusing on urban flooding, human exposure has been a crucial point of concern, as the urban flood vulnerability changes rapidly with time with unforeseen urban growth. Therefore, all the existing methodologies that successfully determine the hazard of urban flooding have failed to determine the level of human exposure to urban flooding, which is the most important parameter of a natural hazard.

Accordingly, researchers encounter several limitations in deriving human exposure levels to a hazard. These include (a) Space and time-consuming approaches in data collection and analysis; (b) Sparse data availability (especially in countries with less open data); (c) Lack of temporal and frequent analyses to trace the rapidly changing urban landscape [7,8,19]; and (d) Lack of an end-user interface i.e., website—for the local community to see the changing risk levels for the local community to be prepared.

2.5. Use of NTL data for urban flood vulnerability mapping

NTL data, which is a satellite observation with the intensity of light at night, can be utilized in determining the urban activity distribution of a particular area. According to Skoufias et al. [10], NTL data has been identified as an economic and population indicator. It is also a temporal set of data that can effectively monitor the rapidly changing urban environment in urban flood-prone areas. Accordingly, NTL data is a unique source of data that can determine the location of human activities, which is not merely the areas with higher population density and built-up areas, which can be derived from primary data collection or satellite images. The contemporary methodologies of identifying urban areas have the limitation of not being able to accurately track the human activity locations; nevertheless, determining the built-up areas.

Urban flood vulnerability levels are determined by two aspects: (a) Flood susceptibility and (b) Human/assets exposure to floods. Flood susceptibility depends on (a) Topographic features: Slope angle, elevation, and aspect ratio [15,26,36]; (b) Weather-related factors: Precipitation [37–39]; (c) Land use and land cover: Normalized Difference Vegetation Index (NDVI) [7,40,41]; (d) River network density [27,42,43]; and, (e) Lithology: Soil texture and moisture [39,44,45].

Although flood susceptibility can be mapped with the aforesaid spatial criteria, mapping human/asset exposure levels to floods has become a hard and time-consuming task, especially in developing countries, due to sparse data availability. For instance, mostly the social and economic damage of the urban flood was studied by calculating the Social Vulnerability Index (SVI), which adopts primary data collection methods within the flood-affected community [7]. As these methods are time-consuming and case-specific, it is important to explore novel approaches to expedite the urban flood vulnerability assessment methods on which this study attempts to be based on. Furthermore, the rapid growth of the urban environments in flood-prone areas, which is a key determinant of human

exposure to urban flooding, also needs to be addressed while overcoming the limitations of the previous studies.

Accordingly, the NTL data is to be used to address the knowledge gap. Here, we attempt to use NTL data to examine the human/asset exposure levels to floods. NTL is a satellite observation method used to sense human activities from night lights, and the observation of Visible and Infrared Imaging Suite (VIIRS) has been available since 2013. The images include the intensity of the light emitted from different sources in the night that indicates the concentration of urban activities. Therefore, VIIRS is to be utilized in the study as a solution to sparse data availability in flood vulnerability mapping in urban areas.

2.6. Interactive web applications

A web application is a representation of the information on a browser interface over the internet. This is a convenient method of delivering any type of data and analysis with easy access and through a user interface that anyone can handle and understand easily. When it comes to geospatial data analysis and representation, a web application can be utilized not only in delivering the results but also in analyzing data at the developer's end and easily used in mapping real-time situations of changing phenomena such as urban flooding [46]. Furthermore, aspects like human exposure to disasters are a type of data that the general public, urban planners, and decision-making authorities should have convenient access to and be accurately available up to date.

Visualizing the urban flood using a web application, which includes the layers with conditioning factors, flood susceptibility and the real-time urban pattern, is crucial in comparing and contrasting the changing effect of urban flood in a specific area and human exposure. Change in both parameters can be seen in the web application and can be used as an effective tool in monitoring the constant change and convenient handling of the user interface. Although there are GIS-based models, HEC-HMS, and HEC-RAS models [47–49] to monitor hydrological behavior and climate change, fewer attempts have been made in monitoring human exposure to urban flooding using a web application: The dataset and its interpretation can be accessed by anyone and for real-time monitoring of the disaster vulnerability.

3. Data and methodology

We intend to measure human exposure to urban flooding using NTL Data focused on the Kelani River basin. This chapter discusses the methodology, data, tools, and techniques used in the study. In the initial stage, the flood susceptibility analysis is done for the Kelani River basin with the aid of past flood occurrences and based on 9 conditioning factors. Then, as the main stage of the study, NTL data is utilized in identifying urban activity hotspots in Kelani River basin, which is validated with the Normalized Urban Area Composite Index (NUACI). Hence, we determine the levels of human exposure to urban flooding.

3.1. Case study area

Kelani River is a critical case in the occurrence of urban flooding in Sri Lanka in which the watershed area is subjected to rapid urban growth and frequent flooding. Kelani River is flooded annually in May and for several years in the months of February and November to an average height

of 3–4 meters near the gauging stations in Nagalagamweediya and Hanwella. According to the flood risk assessment within the Kelani River basin by [50], Hanwella Station is at the highest risk of being inundated, where the water level has risen to 19.7 m in 10 years, which is an increase of 89.3%, and has been subjected to rapid urban growth over the past few years, as revealed from temporal satellite images. Therefore, the Kelani River basin area is an important case study in measuring the level of human exposure to urban flooding. The area of study is derived from the Digital Elevation Model, the Shuttle Radar Topography Mission (SRTM) data downloaded from the USGS Earth Explorer. The extent of the study area is 2298.9 km^2, as depicted in Figure 2.

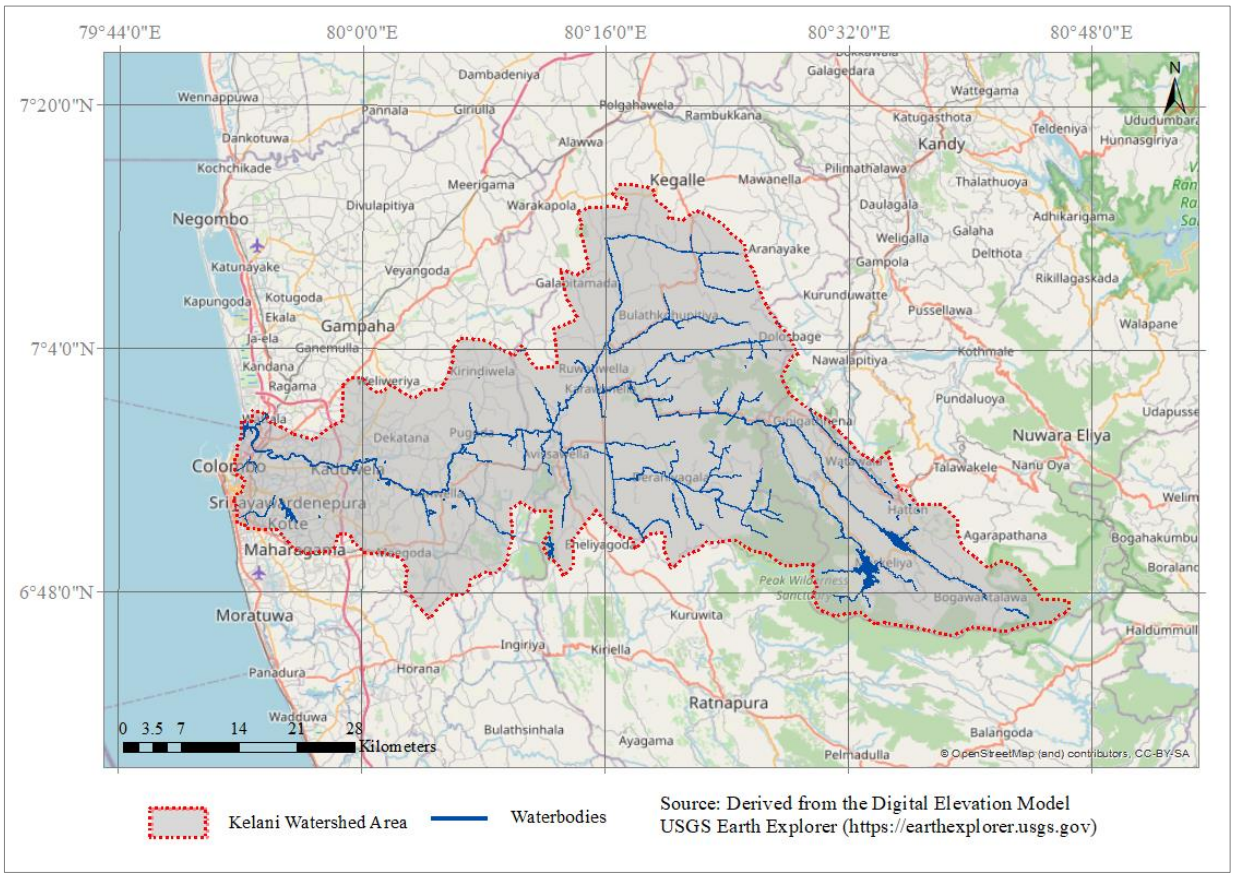

Figure 2. Location of the case study area.

3.2. Methodological framework

The study can be conceptualized as in Figure 3. Accordingly, human exposure to urban flooding is quantified using flood susceptibility analysis and the identification of urban human activities using a novel approach.

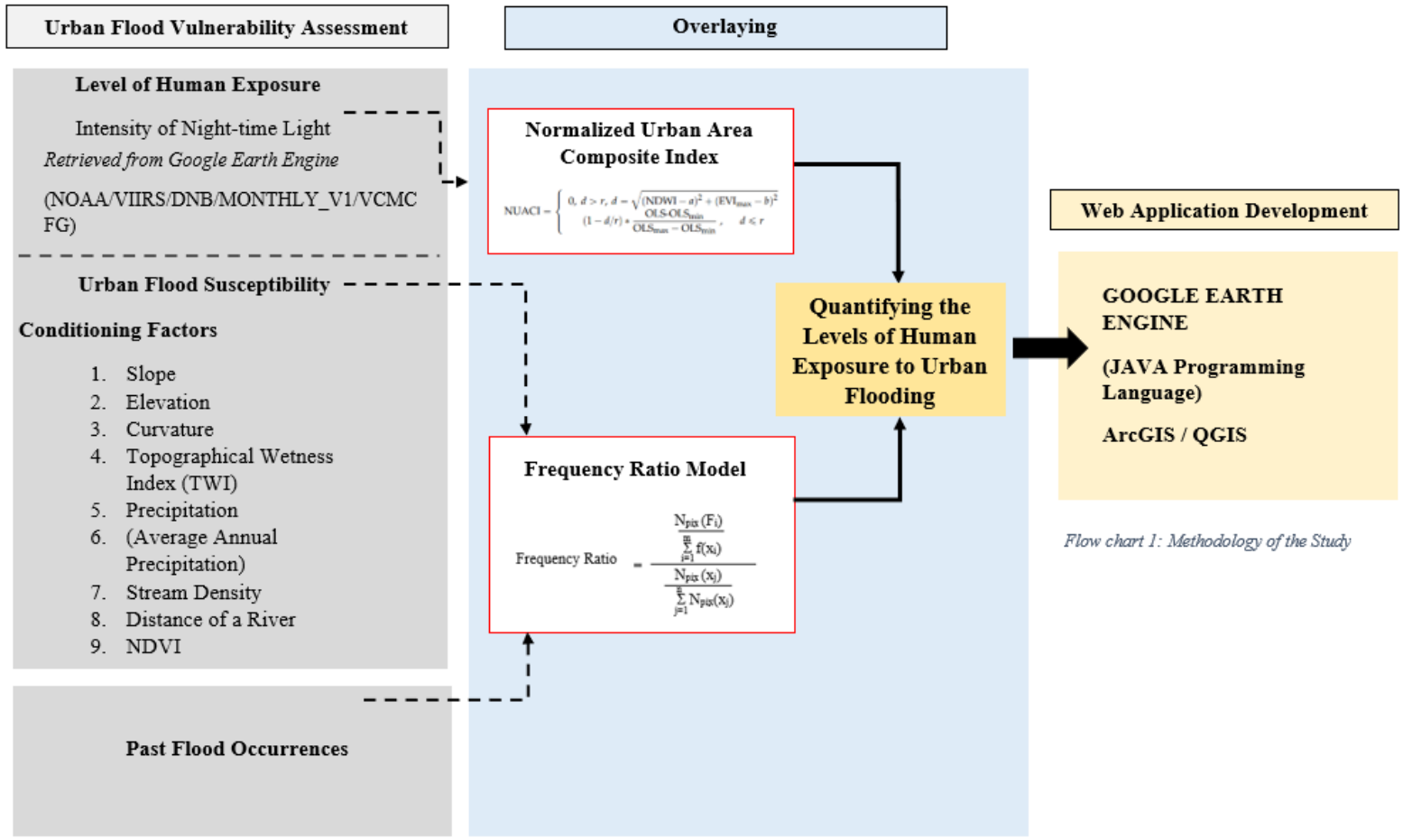

Flow chart 1: Methodology of the Study

Figure 3. Methodology of the study.

3.3. Urban flood vulnerability assessment

3.3.1. Level of human exposure by the intensity of NTL

NTL data is the main source of data used in the study to examine the human exposure levels, which records the brightness of the light emitted artificially from the human activity features. Even though non-urban activities such as agriculture and burning can produce light emissions that can be detected by NTL sensors, urban areas are the primary source of light associated to habitation, land, energy consumption, and other development-related activities. This is because urban regions have most of these activities take place [51]. The NTL is captured using two satellites: The Défense Meteorological Satellite-Program Operational Line Scan System (DMSP-OLS) and Suomi National Polar-orbiting Partnership visible IR Imaging Radiometer Suite (NPP-VIIRS). We utilize monthly composite VIIRS NTL data spanning from 2013 to 2023, retrieved via the GEE, due to its improved spatial resolution and radiometric accuracy compared to DMSP-OLS. A detailed explanation about the data sources used is given in Table S1 of the supplementary documents.

3.3.2. Urban flood susceptibility

According to Khosravi et al. [52], the magnitude of the flood depends on the duration and the intensity of rainfall, while catchment characteristics such as topographic features, land cover, soil characteristics, and river network are the factors affecting flood susceptibility. Accordingly, Table 1 shows the conditioning factors and the attributes considered under each factor for the study. Figure S1 of the supplementary document provides all the maps prepared for each conditioning factor to conduct the spatial analysis.

Table 1. Conditioning factors and the attributes.

Conditioning factor	Attributes	Source of data
Topographic features	Slope	Derived from DEM,
	Elevation	SRTM Data from USGS Earth Explorer
	Curvature	
	Topographical Wetness Index (TWI)	SRTM Data from USGS Earth Explorer
Weather related factors	Precipitation (Average Annual Precipitation)	Meteorological Department, Sri Lanka
Hydrological network	Stream density	Survey Department, Sri Lanka
	Distance of a river	
Land cover	NDVI	Remote Sensing, Landsat 8 data from USGS Earth Explorer
Lithology	Soil type	National Building Research Organization

According to Table 1, topographic features are consisting with Slope, Elevation, Curvature, and Topographical Wetness Index (TWI). Slope is one of the key factors in regional flood analysis in which

the slope angle is the main parameter of study, as the steeper slope results in increased runoff [53]. The slope angle has been categorized into five major classes as 0–5°, 5°–12°, 12°–18°, 18°–30°, and 30°–70°. Elevation is the probability that flood occurrence is lower in high elevations [54]. Accordingly, the elevation map has been taken into analysis and classified into five classes: 0–200 m, 200–500 m, 500–1000 m, 1000–1500 m, and 1500–2500 m. Curvature is also another key indicator in regional flood susceptibility analysis, which reflects the shape of the ground surface [38], as stated in Eq 1. Therefore, a curvature map is derived from the DEM classified into five classes: −4.6–−0.5, −0.5–−0.1, −0.1–0.2, 0.2–0.6, and 0.6–7.5. The Topographical Wetness Index (TWI) is a qualitative representation to evaluate the runoff, which is also a geometric parameter of soil moisture [55], as stated in Eq 2.

$$\text{As} = (\text{flow accumulation} + 1) * \text{cell size}, \tag{1}$$

$$\text{TWI} = \ln(\text{As}/\tan(\beta). \tag{2}$$

'As' is the cumulative upslope area draining through a point (per unit contour length), and tanβ is the slope angle at the point [56]. ArcGIS software was used to produce TWI as classified into 6 classes: 0–8, 8–10, 10–12, 12–15, and 15–25.

Weather-related factors include precipitation. Precipitation is the main factor affecting the magnitude and duration of the flood. Therefore, in flood susceptibility, annual average rainfall for the past five years from 2017 to 2022 has been taken into consideration under five classes: 2000–3500 mm, 3500–4000 mm, 4000–4500 mm, 4500–5500 mm, and 5500–8500 mm. Stream density is also one of the main conditioning factors that contribute to flood occurrence [55]. The density was determined using ArcGIS software, which calculates the stream links per unit area, which is classified into five classes: 1–0.12, 0.12–0.3, 0.3–0.5, 0.5–0.75, and 0.75–1.3.

Hydrological network is a key determinant of flooding. Therefore, the distance from a river link buffer map was also considered in the analysis and classified into five classes, 0–200 m, 200–500 m, 500–1000 m, 1000–2500 m, and 2500–5000 m, to assess the effect of its extent of flooding. The land cover, which determines the level of infiltration and runoff, is a critical factor in urban flooding [38]. NDVI was calculated using Eq 3 given below using the GEE.

$$\text{NDVI} = \frac{\text{NIR Band} + \text{RED Band}}{\text{NIR Band} - \text{RED Band}}. \tag{3}$$

Land cover was examined through NDVI. The NDVI map was created using Operational Land Imager (OLI) sensor images from the Landsat 8 satellite, which were classified into five classes: −0.32–0, 0–0.3, 0.3–0.5, 0.5–0.6, and 0.6–0.8.

Lithology was the last conditional factor, which considered soil type as the main attribute. Soil type also plays a key role in the rate of infiltration, which directly affects the magnitude and extent of flooding, and are classified into the following categories as extracted from the National Building Research Organization soil type mapping: (a) Erosional remnants steep rock, (b) latosols and regosol red and yellow sands, (c) reddish brown latosolic soils, (d) red-Yellow podzolic soils and mountain regosol, (e) red-yellow podzolic soils strongly mottled sub-soils, and (f) red-yellow podzolic soils with prominent A1 or semi-prominent A1.

3.3.3. Past flood occurrences: River gauge data from 2000 to 2021

For past flood occurrences, the extent and the return period are mandatory to analyze future flood

susceptibility [57]. Therefore, the source of past flood occurrences in the Kelani River basin is the daily readings of the river gauges of Kelani River, Hanwella, and Nagalagam Weediya. The data was obtained from the Irrigation Department, Sri Lanka, for the past 21 years from 2000 to 2021. The flood was identified with the daily gauge reading according to Table 2.

Table 2. Flood identification.

Gauging Station	Location	Alert level	Minor flood Level	Major flood level
Hanwella	6.9079, 80.0630	7.00 ft	8.00 ft	10.00 ft
Nagalagam Weediya	6.9579, 9.87862	4.00 ft	5.00 ft	7.00 ft

The average daily water levels from 2000–2021 is depicted in Figure 4. It shows the hourly water levels of the Hanwella and Nagalagam Weediya gauging stations during the flood. This gives a clear representation of the daily flood duration and magnitude. Detailed hourly readings presented in Figure 4 are given in Table S2 and S3 in the supplementary document.

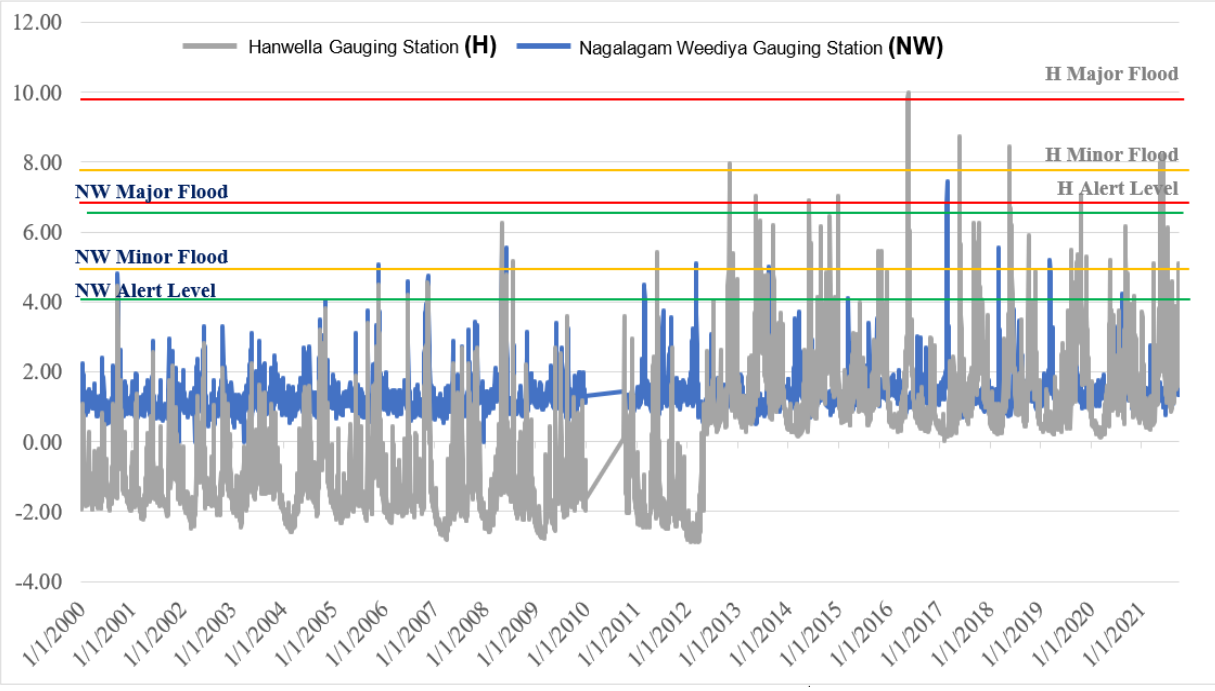

Figure 4. Average water level of gauging stations (Hanwella & Nagalagam Weediya). Source: Irrigation Department, Sri Lanka.

After identifying the flood occurrence using historical gauge data, the spatial extent of past flood events was delineated using Sentinel-1 SAR GRD: C-band Synthetic Aperture Radar data. SAR imagery, with its all-weather, day-and-night acquisition capabilities, enables reliable flood mapping regardless of cloud cover or lighting conditions. For this study, Sentinel-1 SAR data from 2016 to 2022 were retrieved from the GEE platform to identify flood inundation areas corresponding to major flood events within the Kelani River basin. Detailed spatial outputs and processing results are provided in Figure S1 of the supplementary document.

3.4. Overlaying

3.4.1. NUACI

According to Liu et al. [58], the NUACI proposes a new approach to depicting urban activities compared with several indices (Human Settlement Index, Vegetation Adjusted NTL Urban Index), whereas NUACI index given in Eq 4 accounts for the highest accuracy. Therefore, in validating the use of NTL Data in measuring human exposure to urban flooding, NAUCI is utilized.

$$\text{NUACI}=\begin{cases}0, \text{d} > \text{r}, \text{d} = \sqrt{(\text{NDWI}-\text{a})^2 + (\text{EVI}_{\text{max}}-\text{b})^2} \\ (1-\text{d/r}) * \frac{\text{OLS}-\text{OLS}_{\text{min}}}{\text{OLS}_{\text{max}}-\text{OLS}_{\text{min}}}, \text{d} < \text{r}\end{cases}, \quad (4)$$

Note: NDWI—Normalized Difference Vegetation Index; [NWDI (Sentinel 2A) = (NIR − MIR) / (NIR + MIR)]; EVI—Enhanced Vegetation Index; [EVI (Sentinel 2A) = (2.5 * ("NIR Band" – "RED Band"))/("NIR Band" + (2.4 * "RED Band") + 1)]; a—Average Value of NDWI; b—Average Value of EVI; r—Radius of the circle region aggregated with urban samples; d—Distance to the centre of the circle; OLS_{min}—Minimum values in the DMSP-OLS image (VIIRS has been used); OLS_{max}—Maximum values in the DMSP-OLS image (VIIRS has been used).

Accordingly, NUACI ranges between 0–1, which can be utilized in validating the accuracy of using VIIRS in extracting the human activities in an urban area to measure the human exposure to urban flooding.

3.4.2. Frequency Ratio Model (FRM)

The FRM has been used as a bivariate statistical technique that builds up a qualitative relationship between the frequency of flood occurrence and different conditioning factors [27]. The Frequency Ratio is calculated using Eq 5.

$$\text{Frequency Ration} = \frac{\text{Urban Flood Occurrence Ratio}}{\text{The Ratio in each Class in Conditioning Factors}}. \quad (5)$$

Accordingly, the weighted value of the classes used to categorize each parameter is determined based on urban flood occurrence in each class. This method depends on the selection of the required parameters and their categorization into a number of classes, overlaid with the previous flood occurrences at a higher frequency. Finally, the level of susceptibility to flooding in the selected area is determined. Further, Eq 6 was used in weighing each class of the selected conditioning factors that qualitatively determine the level of flood susceptibility. Calculated frequency ration values and prediction ration values are given in Tables S4 and S5 in the supplementary document.

$$\text{Frequency Ratio} = \frac{\frac{\text{N}_{\text{pix}}(\text{F}_\text{i})}{\sum_{\text{i}=1}^{\text{m}} \text{f}(\text{X}_\text{i})}}{\frac{\text{N}_{\text{pix}}(\text{X}_\text{j})}{\sum_{\text{j}=1}^{\text{n}} \text{N}_{\text{pix}}(\text{X}_\text{j})}}. \quad (6)$$

Note: $N_{pix}(F_i)$ = The number of pixels with flood within class i of conditioning factor variable X; $N_{pix}(x_j)$ = The number of pixels within conditioning factor variable; m = The number of classes in the parameter variable; n = The number of factors in the study area.

According to Pradhan et al. [28], the conditional probability of an event to occur, when another past occurrence has been recorded, is the likelihood of that event happening, as stated in the probability theory. Therefore, in calculating the Flood Susceptibility, the conditioning factor layers were reclassified according to the weights obtained by the frequency model, and all the factors are summed up as in Eq 7, where *fr* is the reclassified conditioning factor based on the determined Frequency Ratio weights.

$$\text{Flood Suceptibility} = \text{fr}_1 + \text{fr}_2 + \text{fr}_3 + \text{fr}_4 + \cdots + \text{fr}_\text{n}. \quad (7)$$

3.5. Spatial validation of NTL data and flood susceptibility mapping

To ensure the reliability of the spatial analysis techniques employed in this study, a systematic validation was conducted for both components of the urban flood vulnerability assessment: (a) Flood susceptibility mapping, and (b) identification of urban activity zones using NTL data. In both cases, a confusion matrix framework was applied to quantify the accuracy and predictive performance of the respective models.

3.5.1. Validation of flood susceptibility mapping

The flood susceptibility map generated using the FRM was validated against historical flood event records, including river gauge data and flood extents delineated from Sentinel-1 SAR imagery between 2016 and 2022. This validation involved overlaying known flood occurrence points with model-predicted high-susceptibility zones. A confusion matrix was then constructed to assess the spatial agreement between observed flood areas and predicted flood-prone zones. The matrix categorized spatial pixels into:

- True Positives (TP): Correctly predicted flood-prone areas,
- False Positives (FP): Areas predicted as flood-prone but not observed as flooded,
- True Negatives (TN): Correctly predicted non-flood areas,
- False Negatives (FN): Areas not predicted as flood-prone but observed as flooded.

3.5.2. Validation of NTL-based urban activity detection

In addition to flood susceptibility, the accuracy of using NTL data to detect urban activity intensity was assessed. This was done by comparing the NTL-derived urban zones with the NUACI, a validated benchmark for identifying urban areas, which has an accuracy of 96% according to a study by Tong et al. [59]. Accordingly, the confusion matrix can be simplified as shown in Table 3 and Eq 8.

$$\text{ccuracy} = \frac{\text{TP+TN}}{\text{TP+FP+TN+FN}}. \quad (8)$$

Table 3. Confusion Matrix.

	Predicted Negative	False Negative (FN)
Predicted Positive	True Positive (TP)	False Positive (FP)
Predicted Negative	False Negative (FN)	True Negative (TN)

3.6. Web application development

The web application development was done using the GEE with Java programming language on the developer end, which enables analyzing and visualizing the geospatial information. The key advantage of using GEE in analyzing the data is that the real-time NTL and other satellite image data were incorporated into the study, acquiring the required dates for the analysis on the developer's end easily and can be visualized at the user end, as the human exposure to urban flooding rapidly changes with urban growth and the flood susceptible areas with changing climate patterns, including man-made alterations to the topography of the area. Therefore, we intend to develop a web application that can monitor real-time human exposure to urban flooding with changing external factors. Moreover, this application can be developed for any other location of study with very few input data layers, such as precipitation, soil types, and so on altering the watershed area boundary of the study.

4. Results and discussion

4.1. Level of vulnerability

Figure 5 shows the levels of flood vulnerability for the Kelani watershed area, overlaying the flood susceptible areas and the concentration of human activities, which were derived from the intensity of NTL data.

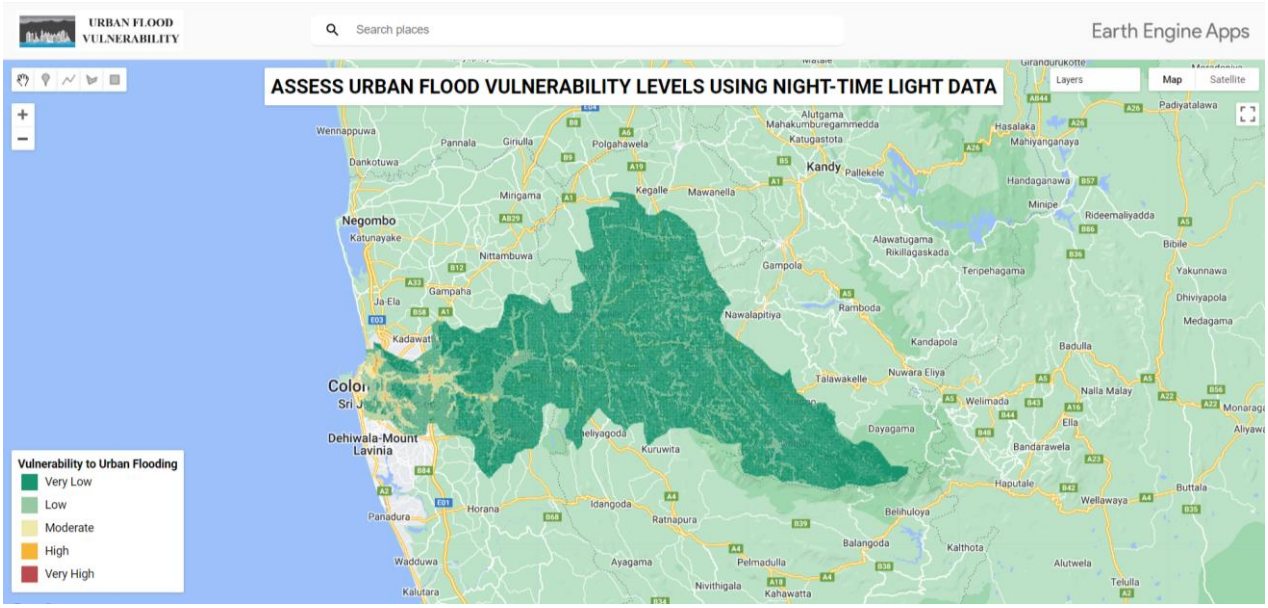

Figure 5. Urban flood vulnerability levels.

4.1.1. Urban areas with very high vulnerability

Figure 6 reveals three highly flood-vulnerable urban spots. These are the (a) Kaduwela; (b) Kelaniya-Peliyagoda; and (c) Kolonnawa-Koswatta corridor.

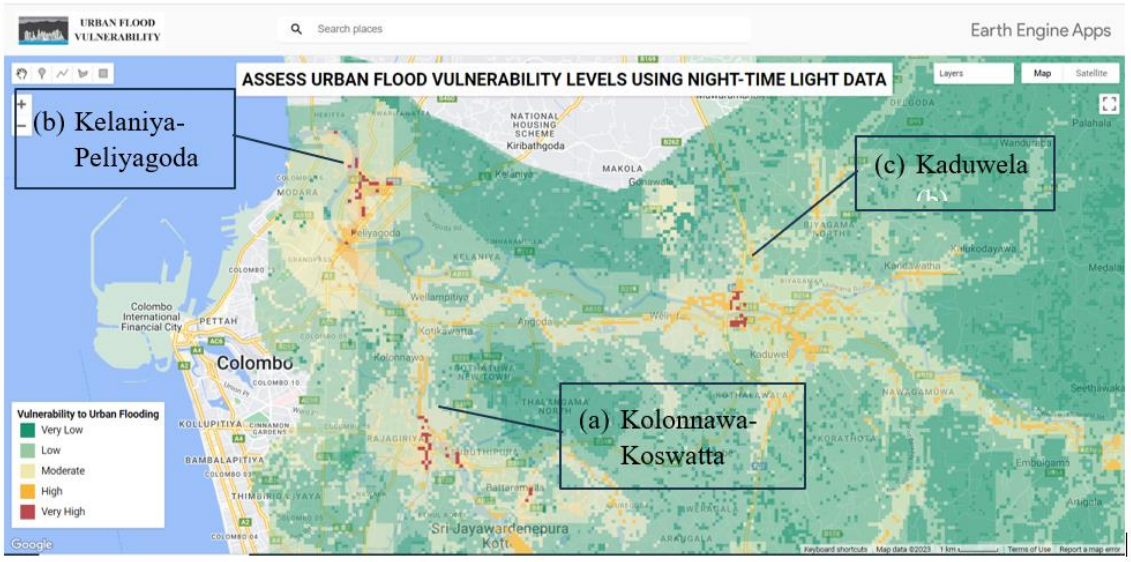

Figure 6. Areas with very high urban flood vulnerability.

Of the three identified urban flood hotspots, severe flooding has been most prominently reported in the Kaduwela area. In this section, we focus on the Kaduwela Municipal Council, a frequently flood-affected region where the magnitude and extent of flooding have increased, as highlighted in the Hydrological Report on the Kelani River Flood in May 2016 by the Irrigation Department of Sri Lanka. According to Ranaweera et al. (2017) [60], the built-up areas of Kaduwela area have increased from 8.6% to 22.9% of the total land use types from 1975 to 2016, which can be clearly observed in Figures 7 and 8. The population increase accounts for +168.9% within that time.

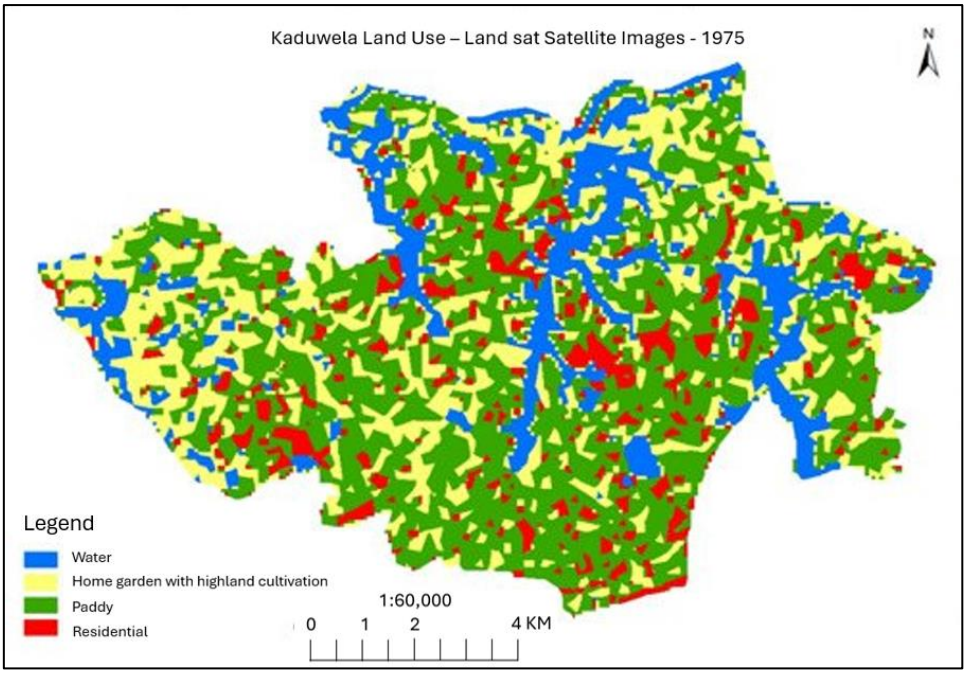

Figure 7. Land use of Kaduwela MC–1975 [60].

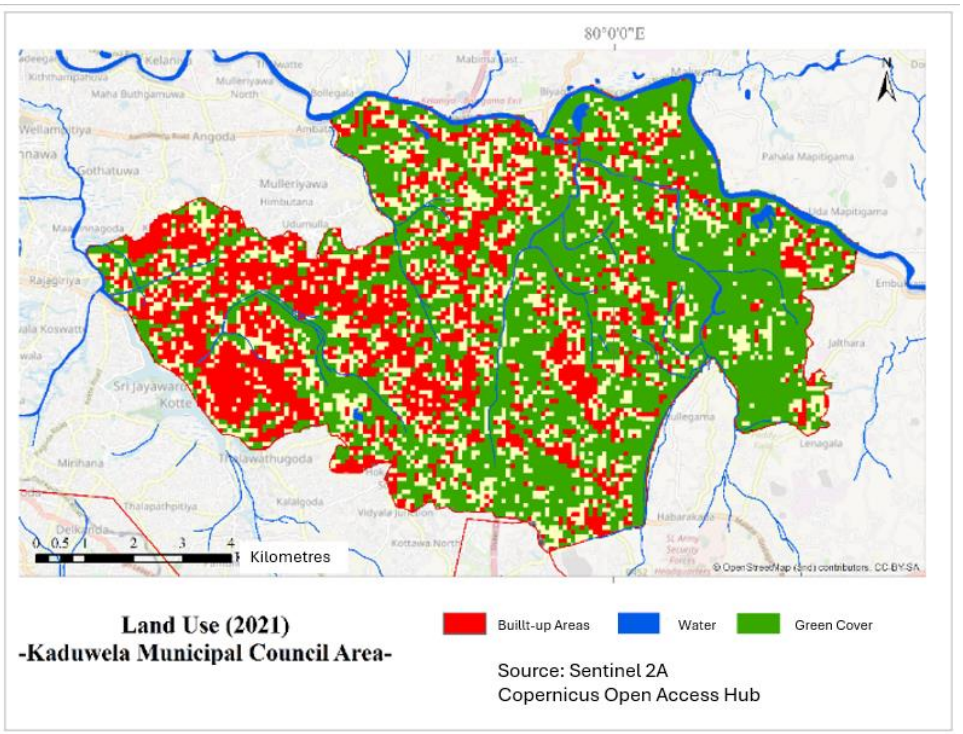

Figure 8. Land use of Kaduwela MC–2021.

Figures 7 and 8 provide a comparative assessment of flood vulnerability in Kaduwela. Figure 9 illustrates urban flood susceptibility based on environmental and topographic conditioning factors, highlighting natural flood-prone areas. In contrast, Figure 10 integrates human exposure by overlaying urban activity indicators such as population density and NTL intensity. This comparison reveals that while natural flood-prone areas are concentrated in low-lying regions near water bodies, human exposure is significantly higher in dense urban settlements, commercial hubs, and industrial zones, emphasizing the role of land-use transformation in increasing flood risk.

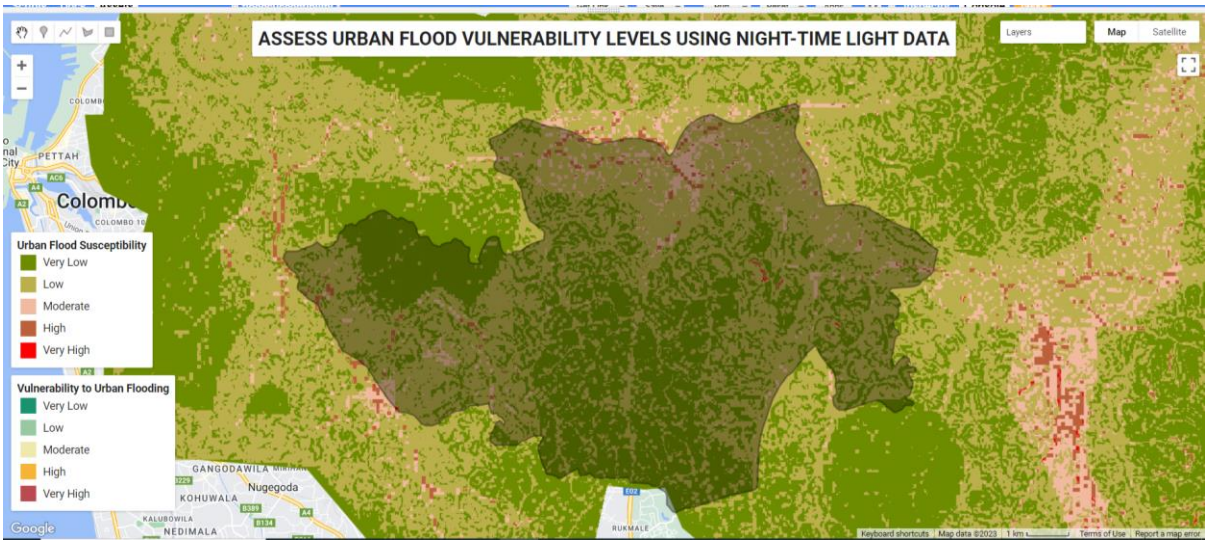

Figure 9. Urban flood susceptibility levels—Kaduwela.

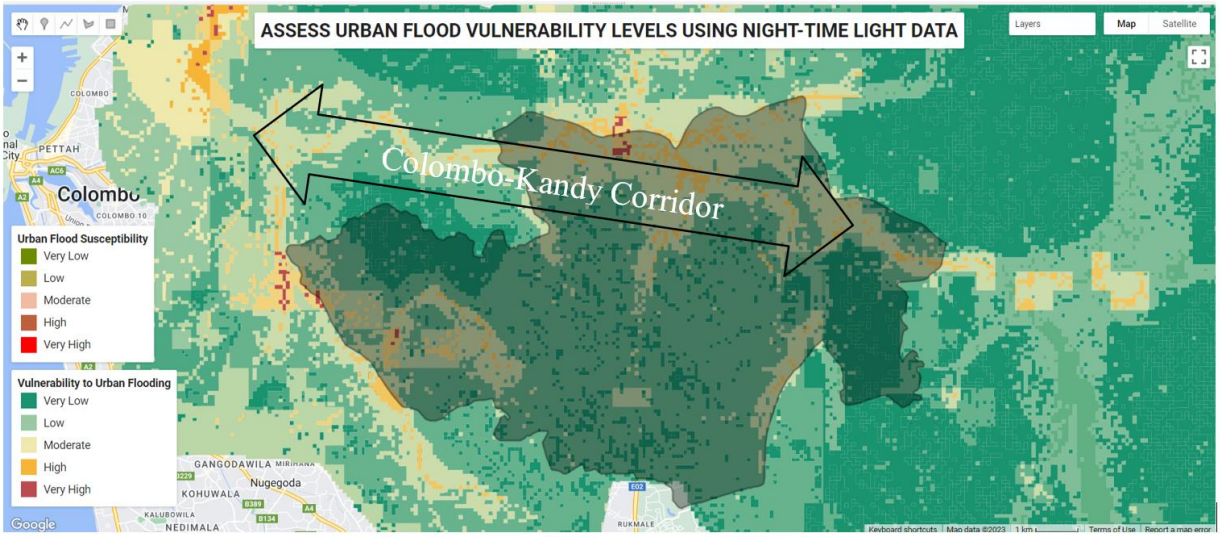

Figure 10. Human exposure to urban flooding—Kaduwela.

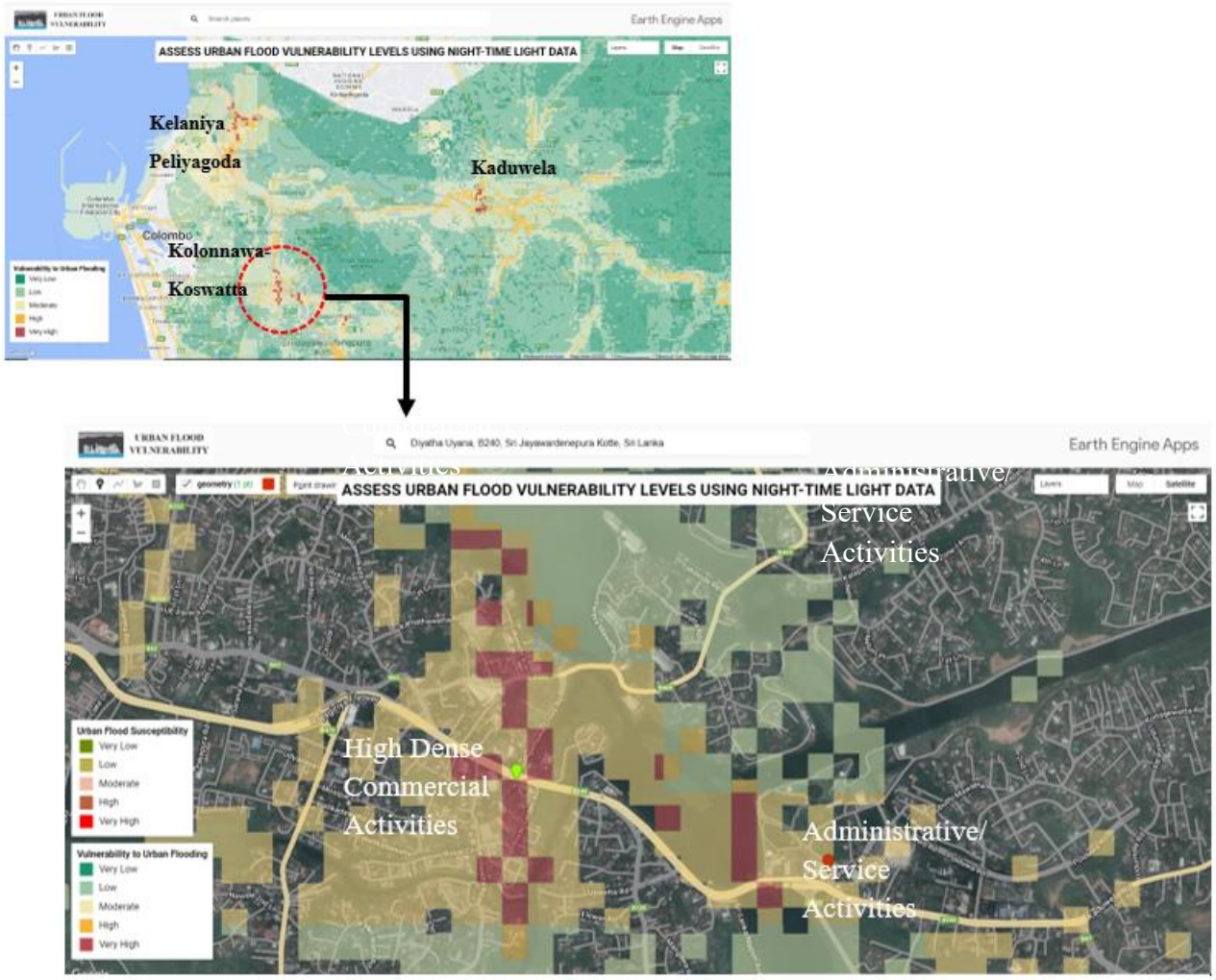

Figure 11. Battaramulla—High urban flood vulnerable area.

With the construction of the outer-circular expressway in 2014, Kaduwela is a rapidly growing urban hotspot in the Colombo-Kandy corridor (Figure 10). Furthermore, the Kaduwela-Malabe area has been identified as an Information Technology, High-Tec business development zone with the existing economic setting of the area, which attracts thousands of professionals to the city, according to the studies done by the Colombo Megapolis Development Plan.

Moving on to the Kolonnawa-Koswatta corridor (a), this region has experienced significant urbanization, contributing to increased vulnerability to flooding. Similarly, the Kolonnawa-Koswatta area is a developing economic-service center for Colombo, with the location of administrative activities.

Figure 11 illustrates the urban flood vulnerability of the Battaramulla area, a highly densified corridor with significant commercial, administrative, and service activities. Over time, these developments have contributed to an increase in urban flood vulnerability, as seen in the map's red zones. Additionally, the population in the surrounding Kolonnawa-Koswatta area has surged by 172.5% from 1975 to 2016, exacerbating the flood risk. With this rapid growth, the already vulnerable area faces even more challenges, particularly with frequent flooding events. For example, during the October 2022 flood, Kolonnawa recorded the highest number of displaced people, with a total of 3,666 individuals affected.

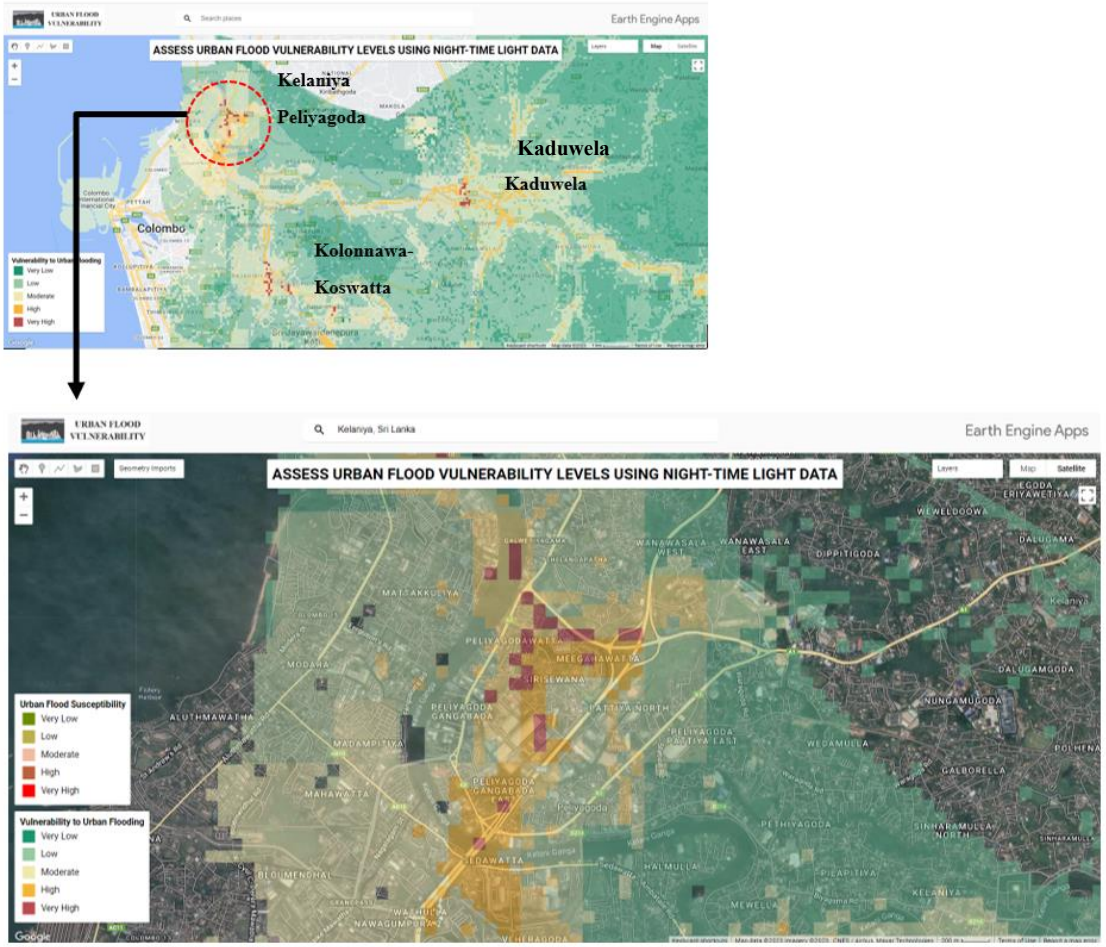

Figure 12. Peliyagodawatta—High urban flood vulnerable area.

Figure 12 shows that the Kelaniya-Peliyagoda area is the third hotspot having high urban flood vulnerability, as indicated by our results. The map highlights significant regions with high to very high flood vulnerability, particularly in areas such as Peliyagoda, where dense development and low-lying land contribute to the increased risk. This heightened vulnerability is reflected in the color-coded zones on the map, where the red and orange areas represent the most susceptible locations to urban flooding.

The population change of the Kelaniya-Peliyagodawatta area is +57.1% from 1975 to 2016, which is comparatively lower than the other two (Kaduwela and Kolonnawa-Koswatta Corridors) identified as very high flood-vulnerable hotspots, according to the study. This is a clear reflection of the increasing urbanization and development within the region, which has elevated the flood risk in this area. The population growth in the Kelaniya-Peliyagoda area is a key factor contributing to the increased vulnerability. From 1975 to 2016, the population rose by 57.1%. This is comparatively lower than the growth rates observed in the Kadawela and Kolonnawa-Koswatta corridors, which are also identified as high flood-risk hotspots. However, the population increase in the Kelaniya-Peliyagoda area has brought with it a greater human exposure to flood risks. The development in this area is not limited to residential growth; new infrastructure projects and expanding economic activities further intensify the flood vulnerability.

As shown in the Figure 12, the higher vulnerability zones are associated with areas of significant commercial, residential, and service infrastructure. This suggests that the developments in the Peliyagoda-Kelaniya region, which include new commercial centers, housing, and industrial areas, have likely contributed to the exacerbation of urban flood risks. Our findings highlight the need for targeted urban planning and flood mitigation strategies to address the growing flood vulnerability in this corridor.

4.1.2. Urban areas with high vulnerability

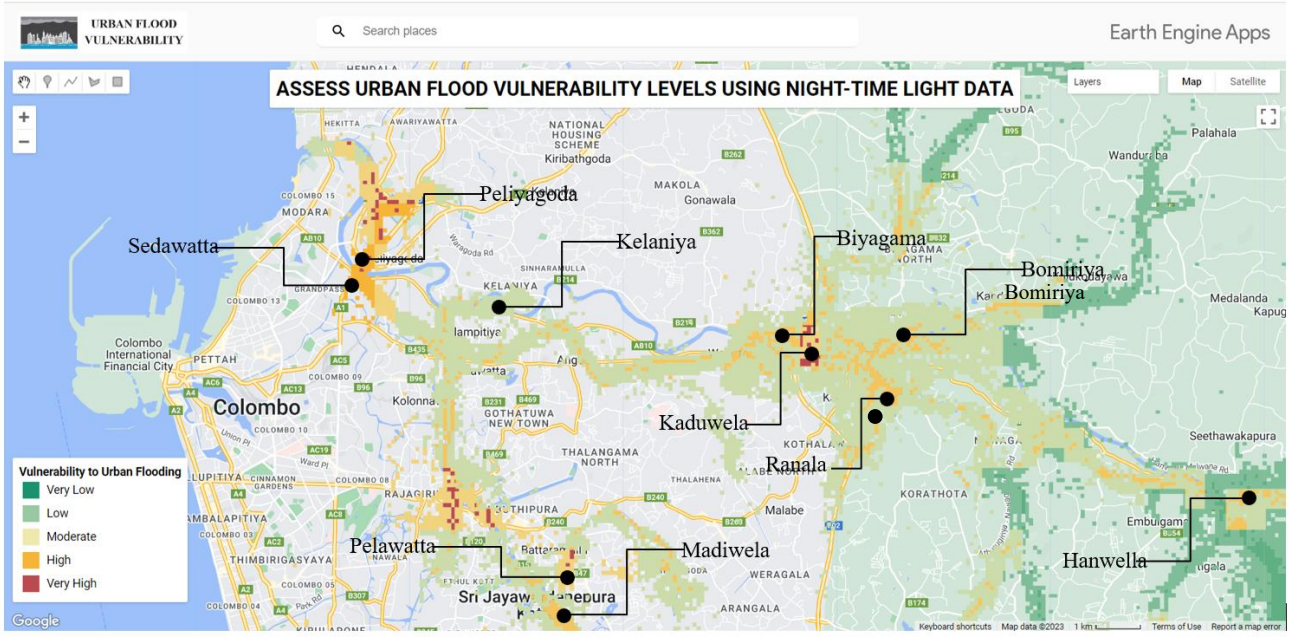

Figure 13. Areas with high urban flood vulnerability.

Figure 13 highlights the areas with high urban flood vulnerability, shown in orange on the map. These areas include the urban cores of Peliyagoda-Kelaniya, Kolonnawa-Koswatta, and Kaduwela, as well as the surrounding regions such as Madiwala, Pelawatta, Sedwatta, Biyagama, Ranala, Bomiriya, and Hanwella. According to the study, these locations are highly vulnerable to urban flooding.

Focusing on the Hanwella area, which is another significant hotspot for urban flooding, the population increased from 1975 to 2016 by 25.1%. This growth rate is comparatively lower than the more heavily affected areas like Peliyagoda-Kelaniya and Kolonnawa-Koswatta. However, the results suggest that the increased human density in these areas has intensified the vulnerability to flooding. This finding emphasizes the importance of understanding the relationship between population growth and flood vulnerability, highlighting that the level of human exposure to urban flooding is closely linked to the scale of urban development and population density, which significantly impacts flood risk.

4.1.3. Urban areas with moderate vulnerability

Figure 14 indicates the areas with moderate flood vulnerability in yellow. The moderate urban flood vulnerability includes the flood susceptible areas and the intensity of night light that represents the concentration of urban activities. The moderate flood vulnerable areas include the high and moderate flood susceptible areas with a moderate concentration of urban activities, according to the intensity of NTL. This mostly includes the adjacent area to high urban flood vulnerable areas.

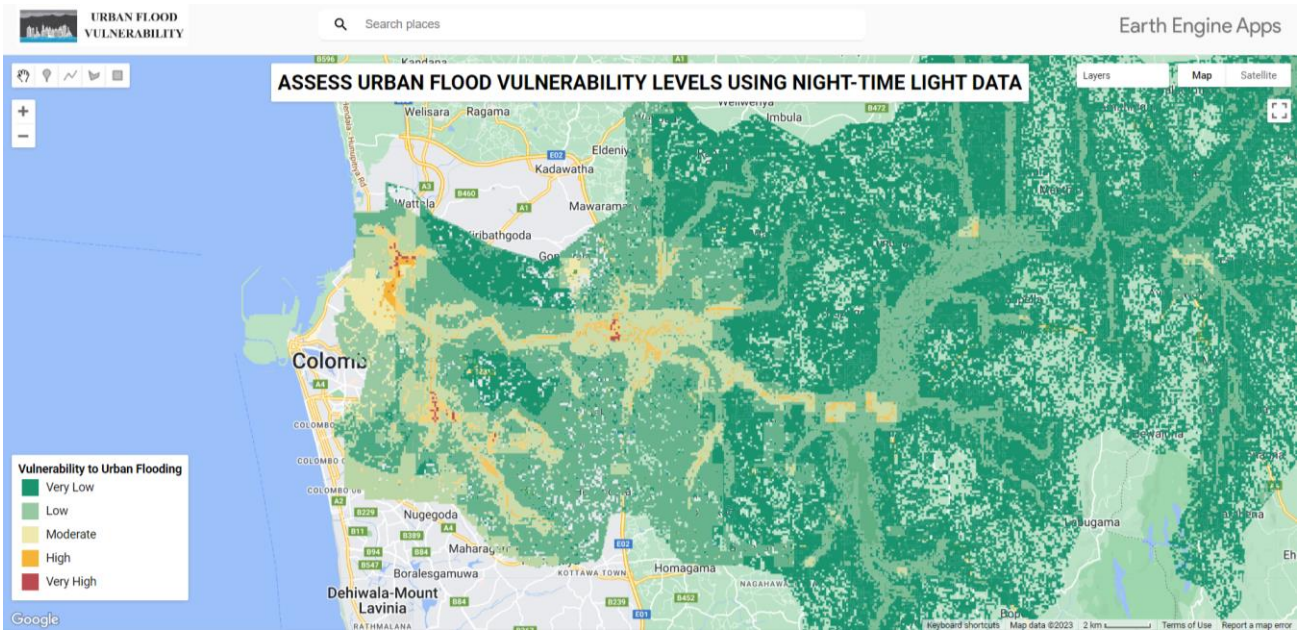

Figure 14. Areas with moderate urban flood vulnerability.

4.1.4. Urban areas with low and very low flood vulnerability

Figure 15 presents the urban areas in the Kelani Watershed Basin that exhibit low and very low flood vulnerability. These areas, marked in light green and dark green on the map, are characterized

by minimal flood risk, which can be attributed to factors such as elevated terrain, lower urbanization, and minimal human activity.

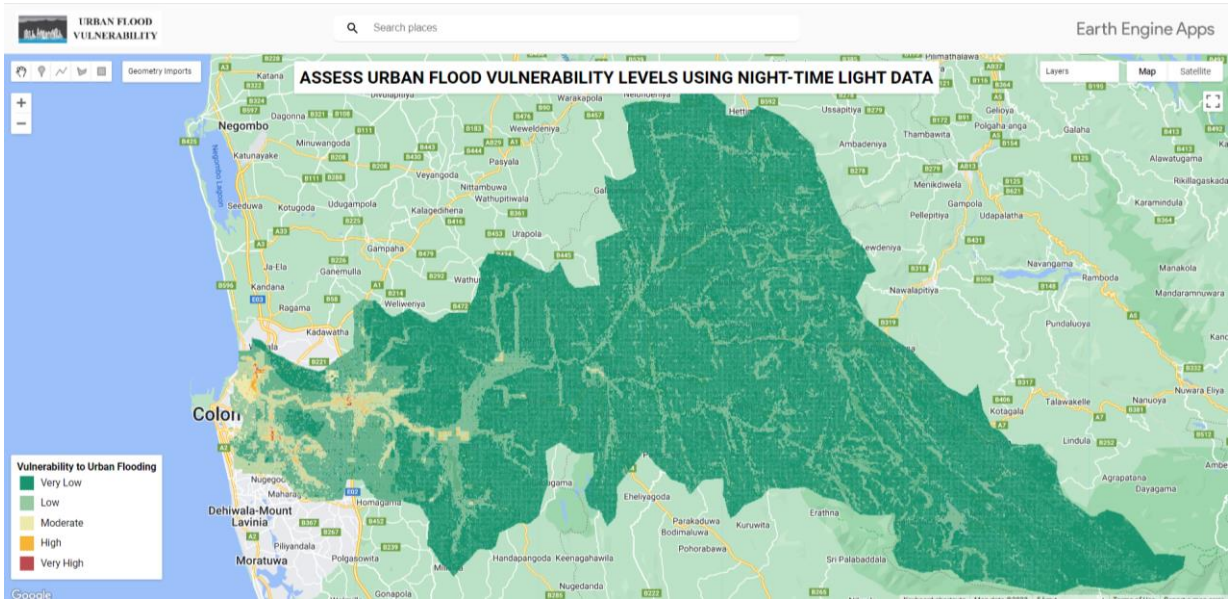

Figure 15. Areas with low and very low urban flood vulnerability.

4.1.5. Influence of urban activity concentration on flood vulnerability

In contrast to the areas with low and very low flood vulnerability, the concentration of urban activities plays a crucial role in determining the flood susceptibility of certain regions. Areas with higher urban activity concentrations, as indicated by NTL data, tend to exhibit higher vulnerability to urban flooding. The more densely populated and developed areas, which are typically characterized by extensive infrastructure and urbanization, contribute to increased flood risk due to factors such as reduced natural drainage capacity, impervious surfaces, and the presence of critical infrastructure that can exacerbate the impact of flooding.

Both areas marked in the maps (Figures 16 and 17) are diagnosed with higher flood susceptibility. However, the area marked in red shows a higher vulnerability to urban flooding, while the area marked in blue shows a lower vulnerability to urban flooding. This discrepancy can be attributed to the concentration of urban activities. The intensity of NTL data reveals that the blue-marked area, where no human activities are recorded, has a lower flood vulnerability. In contrast, the red-marked area, with a higher concentration of urban activities, shows higher flood vulnerability. Despite both areas being highly susceptible to urban flooding, the higher urbanization in the red-marked area contributes to its increased vulnerability.

The maps in Figures 16 and 17 illustrate this relationship, with Figure 16 focusing on flood susceptibility and Figure 17 showing human exposure to flooding in regions with varying levels of urban activity.

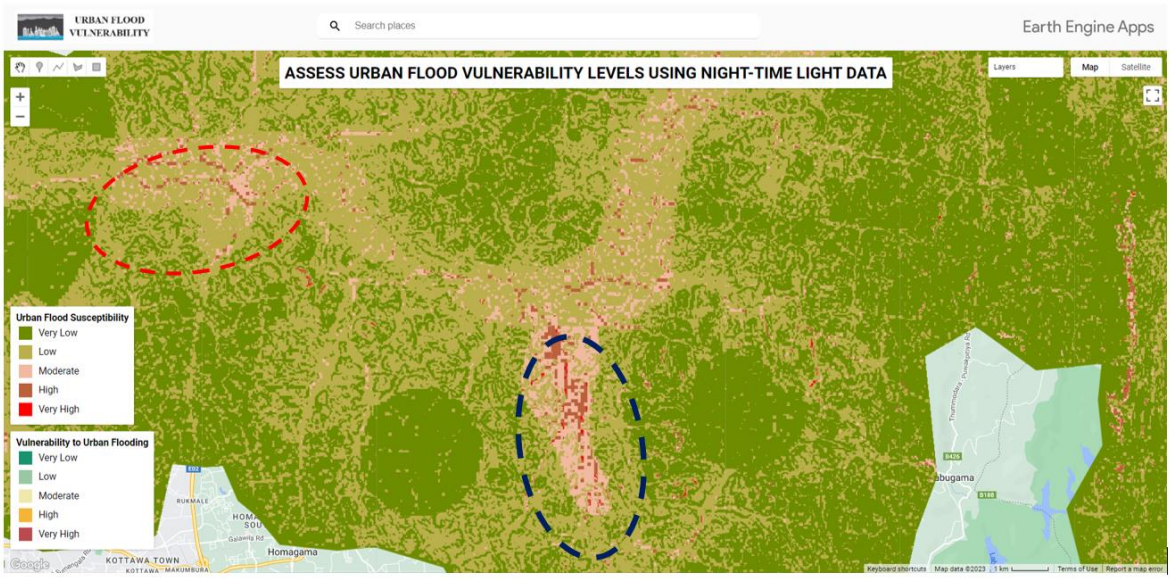

Figure 16. Flood susceptibility—Hanwella area.

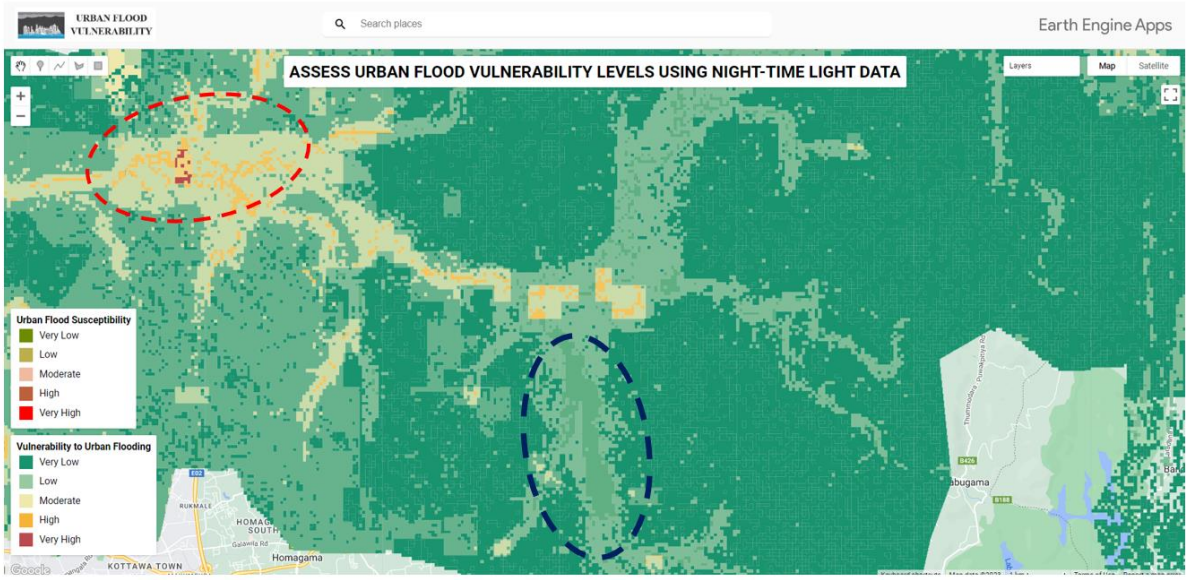

Figure 17. Human exposure to urban flooding—Hanwella area.

4.1.6. Advantages of using NTL in vulnerability assessments

NTL, which has been the novel source of data used in this study, is vital as an indicator of urban activities in quantifying the urban flood vulnerability. A key advantage of NTL is the availability of real-time data monthly. When compared with the other urban area identifying calculations such as NDVI, NDBI, and EVI, the data has to be acquired for a specific date considering the availability of Landsat or Sentinel images, the sparse data availability, and disturbances with cloud cover affecting the accuracy of those contemporary methods to extract the urban built-up data. As specified, those indices are for extracting 'urban built-up', not specifically the 'urban activities', which directs us to

the next key advantage of NTL, which has been an effective measure to determine the urban activities. The other main advantage is NTL's convenience in further analysis, as the intensity level of the NTL data is considered, and no calculations are required as in the discussed indices to determine the urban activities. Therefore, NTL can be used, conveniently, effectively, accurately as a measure to determine the distribution of urban activities of a specific area.

4.2. Development of a web application

The web application was developed using Java programming language and GEE, enabling real-time urban flood vulnerability assessments based on NTL data. The developed web application can be found in: https://researchnuwanidata.users.earthengine.app/view/floodvulnerability.

The web application incorporates data layers related to flood susceptibility, which include the nine conditioning factors, including Slope, Elevation, Curvature, Topographical Wetness Index (TWI), Precipitation, Stream Density, Distance of a River, NDVI, and Soil Type. These data layers were retrieved from remote sensing sources and integrated into the platform as extensively discussed in the methodology section. The past flood occurrences for the Kelani River basin, determined using historical data from the Irrigation Department of Sri Lanka, were also included to assess flood susceptibility across the study area.

The key advantage of using the GEE for this application is the ability to access and analyze large datasets, such as NTL and conditioning factors, seamlessly. Real-time data updates are easily incorporated, enabling continuous monitoring and analysis of flood vulnerability. The web application can be customized by users, enabling them to select specific data layers for analysis. The user interface is designed to be simple and user-friendly, with an interactive map that provides various tools such as zoom, legend, map marker, and shape tools for a more detailed examination of the area.

In the application, the flood susceptibility of the Kelani River basin is visualized alongside the NTL data, which represents human activity intensity. The integration of NTL data, which captures the concentration of urban activities at night, enables an accurate assessment of human exposure to flood risks. The analysis was validated using the NUACI, providing a clear indication of the intensity and distribution of urban activities.

Users can easily interact with the platform by switching between different map layers to visualize and compare the flood susceptibility and human exposure to flooding. Additionally, the application includes both satellite maps and open street maps, which can be toggled for better visualization and analysis. These features make the platform an invaluable tool for urban planners, policymakers, and disaster risk managers, offering a comprehensive view of urban flood vulnerabilities in the study area.

Furthermore, the web application is designed to be adaptable to other regions. By simply altering the boundary of the study area and adjusting the data layers, the platform can be used to assess flood vulnerability in different watersheds, considering the specific characteristics and past flood occurrences of each region. This flexibility makes the web application a powerful tool for decision-making and real-time monitoring of urban flood risks.

In conclusion, this web application serves as an effective decision-making tool for urban planning, enabling stakeholders to monitor and mitigate the risks associated with urban flooding. The ability to update NTL data in real-time and overlay it with other flood susceptibility factors ensures that the application provides up-to-date, actionable insights for managing flood risks and planning for future urban development.

4.3. Spatial validation results

4.3.1. Flood susceptibility model accuracy

The flood susceptibility map was validated using spatial overlays with confirmed flood occurrences from 2016–2022, derived from SAR-based flood extents and gauge station records. The confusion matrix analysis produced an overall accuracy of 82%, indicating a strong agreement between predicted and observed flood-prone areas.

4.3.2. NTL classification accuracy

The NTL-derived urban activity map was validated using NUACI as a reference. This comparison, also based on a confusion matrix, produced an accuracy of 76%, reinforcing the utility of NTL data for exposure mapping, despite limitations in detecting smaller, low-light urban settlements.

4.4. Limitations

While this study introduces a novel approach to urban flood vulnerability mapping using NTL data, several limitations must be acknowledged. First, the classification accuracy of NTL-derived urban activity zones, although validated using NUACI with 76% accuracy, can be further improved by integrating higher-resolution socio-economic or mobile sensing data. Second, the spatial resolution of VIIRS NTL data may limit the detection of micro-scale urban dynamics, particularly in heterogeneous urban environments. Third, the web application depends on monthly composite NTL datasets, which may not fully capture daily variations in urban activity or emergency events. Additionally, although a confusion matrix-based validation was applied to assess both flood susceptibility and urban exposure models, field-based ground truth validation was not conducted. We acknowledge the importance of empirical verification and recommend incorporating ground-reported flood data and participatory validation in future studies to enhance predictive robustness. Finally, incorporating real-time hydrological data and forecast models could improve the temporal responsiveness of flood risk assessment. In the future, researchers should also focus on enhancing the web interface to support real-time alerts and participatory data inputs for decision-making.

5. Conclusions

We propose a methodology for quantifying human exposure to urban flooding using NTL data. Urban flood vulnerability is evaluated through two aspects: (a) Flood susceptibility, which assesses the likelihood of flood occurrence, and (b) exposure, represented by the concentration of human activities, which is measured using NTL intensity. The Kelani River watershed was used as a case study, where higher NTL intensity correlated with areas of intense urban activity, indicating greater human exposure to flood risks.

Flood susceptibility was quantified using nine conditioning factors, including slope, elevation, curvature, topographic wetness index, average annual precipitation, land cover, stream network density, distance to streams, and soil types. These factors were integrated with past flood occurrences using the FRM, which successfully identified flood-prone areas. Researchers have validated the FRM model's

effectiveness, with an accuracy of over 90% in flood hazard mapping. In this study, the FRM approach accurately quantified flood susceptibility in the Kelani River watershed.

NTL data, which is often used to map urbanized areas, was employed to assess human exposure to flooding. The results indicate that areas with higher NTL intensity correspond to higher flood susceptibility, with urbanized areas showing increased vulnerability. Conversely, areas with lower NTL intensity, such as wetlands and marshes, exhibit lower human exposure, despite their higher flood susceptibility, highlighting the importance of incorporating both susceptibility and exposure into flood vulnerability assessments. The use of the NUACI for classifying urban activity concentration showed high accuracy (96%) in previous studies. In this study, the classification of NTL data achieves 76% accuracy, and researchers should focus on improving this classification precision for more accurate flood vulnerability mapping.

The developed web application provides a user-friendly platform for real-time flood vulnerability assessment and urban planning. The application enables users to select and visualize various data layers, such as flood susceptibility and human exposure, with real-time updates. Its adaptability makes it a useful tool for other regions, supporting flood risk monitoring and decision-making. The flexibility to update the data sources and visualize urban flood vulnerability ensures its ongoing relevance for urban planners, disaster managers, and policymakers. This study contributes a cost-effective, time-efficient, and open-source methodology that addresses many limitations found in previous research. The approach combines NTL data with flood susceptibility factors to provide a comprehensive understanding of urban flood vulnerability. Moving forward, enhancing the precision of NTL classification and incorporating real-time data into flood exposure warning systems could further improve flood risk management. This methodology can be expanded to other regions for monitoring urban flood vulnerability and guiding urban planning and risk reduction strategies in flood-prone areas.

Use of AI tools declaration

The authors declare they have not used Artificial Intelligence (AI) tools in the creation of this article.

Acknowledgements

The authors sincerely thank the reviewers and editors for their constructive feedback and valuable suggestions.

Conflict of interest

The authors declare no conflicts of interest.

Author's contribution

Nuwani Kangana and Nayomi Kankanamge; Conceptualization, and methodology, Nuwani Kangana; formal analysis, and writing—original draft preparation, Nayomi Kankanamge; writing—review and editing, supervision.

References

1. Yao L, Chen L, Wei W (2017) Exploring the linkage between urban flood risk and spatial patterns in small urbanized catchments of Beijing, China. *Int J Environ Res Public Health* 14: 239. https://doi.org/10.3390/ijerph14030239
2. CRED, UNDRR (2020) Human cost of disasters: An overview of the last 20 years (2000–2019). Available from: https://www.undrr.org/publication/human-cost-disasters-overview-last-20-years-2000-2019.
3. Kankanamge N, Yigitcanlar T, Goonetilleke A, et al. (2020) Determining disaster severity through social media analysis: Testing the methodology with South East Queensland Flood tweets. *Int J Disaster Risk Reduct* 42: 101360. https://doi.org/10.1016/j.ijdrr.2019.101360
4. Alahacoon N, Matheswaran K, Pani P, et al. (2018) A decadal historical satellite data and rainfall trend analysis (2001–2016) for flood hazard mapping in Sri Lanka. *Remote Sens* 10: 448. https://doi.org/10.3390/rs10030448
5. Kankanamge N, Yigitcanlar T, Goonetilleke A, et al. (2019) Can volunteer crowdsourcing reduce disaster risk? A systematic review of literature. *Int J Disaster Risk Reduct* 35: 101197. https://doi.org/10.1016/j.ijdrr.2019.101097
6. Agonafir C, Lakhankar T, Khanbilvardi R, et al. (2023) A review of recent advances in urban flood research. *Water Secur* 19: 100141. https://doi.org/10.1016/j.wasec.2023.100141
7. Tate E, Rahman MA, Emrich C T, et al. (2021) Flood exposure and social vulnerability in the United States. *Nat Hazards* 106: 435–457. https://doi.org/10.1007/s11069-020-04470-2
8. Smith A, Bates PD, Wing O, et al. (2019) New estimates of flood exposure in developing countries using high-resolution population data. *Nat Commun* 10: 1814. https://doi.org/10.1038/s41467-019-09282-y
9. Weerasinghe KM, Gehrels H, Arambepola N, et al. (2018) Qualitative Flood Risk assessment for the Western Province of Sri Lanka. *Procedia Eng* 212: 503–510. https://doi.org/10.1016/j.proeng.2018.01.065
10. Skoufias E, Strobl E, Tveit T (2021) Can we rely on VIIRS nightlights to estimate the short-term impacts of natural hazards? Evidence from five South East Asian countries. *Geomat Nat Haz Risk* 12: 381–404. https://doi.org/10.1080/19475705.2021.1879943
11. Chen Y, Zhou H, Zhang H, et al. (2015) Urban flood risk warning under rapid urbanization. *Environ Res* 139: 3–10. https://doi.org/10.1016/j.envres.2015.02.028
12. Hsu FC, Baugh KE, Ghosh T, et al. (2015) DMSP-OLS radiance calibrated nighttime lights time series with intercalibration. *Remote Sens* 7: 1855–1876. https://doi.org/10.3390/rs70201855
13. Lin CY, Ackerman A, Johnston D, et al. (2022) LiDAR operation and digital modeling visualization to communicate stormwater management at green spaces in developing regions. *Eurographics Association*. https://doi.org/10.2312/envirvis.20221056
14. Rahman MR, Thakur PK (2018) Detecting, mapping and analysing of flood water propagation using synthetic aperture radar (SAR) satellite data and GIS: A case study from the Kendrapara District of Orissa State of India. *Egypt J Remote Sens Space Sci* 21: S37–S41. https://doi.org/10.1016/j.ejrs.2017.10.002
15. Cao R, Li F, Feng P (2020) Exploring the hydrologic response to the urban building coverage ratio by model simulation. *Theor Appl Climatol* 140: 1005–1015. https://doi.org/10.1007/s00704-020-03139-x

16. Kankanamge N, Yigitcanlar T, Goonetilleke A (2021) Public perceptions on artificial intelligence driven disaster management: Evidence from Sydney, Melbourne and Brisbane. *Telemat Inform* 65: 101729. https://doi.org/10.1016/j.tele.2021.101729
17. Marolla C (2024) Urban flood resilience: Risk and business continuity management systems strategic approach. *J Clin Epidemiol Public Health* 2: 1–13. https://doi.org/10.33774/coe-2024-rjg0b
18. Paudel S, Benavides JC (2023) *Flood Ecology*, Oxford: Oxford University Press. https://www.sci-hub.ru/10.1093/obo/9780199830060-0244
19. Kumar D, Bhattacharjya RK (2020) Review of different methods and techniques used for flood vulnerability analysis. *Nat Hazards Earth Syst Sci Discuss* 1: 1–15, https://doi.org/10.5194/nhess-2020-297, 2020
20. Sy HM, Luu C, Bui QD, et al. (2023) Urban flood risk assessment using Sentinel-1 on the Google Earth Engine: A case study in Thai Nguyen city, Vietnam. *Remote Sens Appl: Soc Environ* 31: 1100987. https://doi.org/10.1016/j.rsase.2023.100987
21. Shinde S, Pande CB, Barai VN, et al. (2023) Flood impact and damage assessment based on the Sentinel-1 SAR data using Google Earth Engine, In: *Climate Change Impacts on Natural Resources, Ecosystems and Agricultural Systems*, 483–502. https://doi.org/10.1007/978-3-031-19059-9_20
22. Gemitzi A, Kopsidas O, Stefani F, et al. (2024) A constantly updated flood hazard assessment tool using satellite-based high-resolution land cover dataset within Google Earth Engine. *Land* 13: 1919. https://doi.org/10.3390/land13111929
23. Prasertsoong N, Puttanapong N (2025) An integrated framework for satellite-based flood mapping and socioeconomic risk analysis: A case of Thailand. *Prog Disaster Sci* 25: 100393. https://doi.org/10.1016/j.pdisas.2024.100393
24. Asian Disaster Reduction Center (2021) Natural Disaster Databook 2021: An Analytical Overview. Available from: https://www.preventionweb.net/publication/natural-disasters-data-book-2021-analytical-overview.
25. Bagheri A, Liu GJ (2025) Climate change and urban flooding: assessing remote sensing data and flood modeling techniques: A comprehensive review. *Environ Rev* 33: 1–14. https://doi.org/10.1139/er-2024-0065
26. Vojtek M, Vojteková J (2019) Flood susceptibility mapping on a national scale in Slovakia using the analytical hierarchy process. *Water* 11: 364. https://doi.org/10.3390/w11020364
27. Samanta S, Pal DK, Palsamanta B (2018) Flood susceptibility analysis through remote sensing, GIS and frequency ratio model. *Appl Water Sci* 8: 66. https://doi.org/10.1007/s13201-018-0710-1
28. Pathak S, Panta HK, Bhandari T, et al. (2020) Flood vulnerability and its influencing factors. *Natl Hazards* 104: 2175–2196. https://doi.org/10.1007/s11069-020-04267-3
29. Kates RW (1971) Natural hazard in human ecological perspective: Hypotheses and models. *Econ Geogr* 47: 438–451. https://doi.org/10.2307/142820
30. Birkmann J, Schüttrumpf H, Handmer J, et al. (2023) Strengthening resilience in reconstruction after extreme events—Insights from flood affected communities in Germany. *Int J Disaster Risk Reduct* 96: 103965. https://doi.org/10.1016/j.ijdrr.2023.103965
31. Balica SF, Wright NG, van der Meulen F (2012) A flood vulnerability index for coastal cities and its use in assessing climate change impacts. *Nat Hazard* 64: 73–105. https://doi.org/10.1007/s11069-012-0234-1

32. Blistanova M, Zelenakova M, Blistan P, et al. (2016) Assessment of flood vulnerability in Bodva river basin, Slovakia. *Acta Montan Slovaca* 21: 19–28. https://doi.org/10.3390/ams21010019
33. Skougaard Kaspersen P, Høegh Ravn N, Arnbjerg-Nielsen K, et al. (2017) Comparison of the impacts of urban development and climate change on exposing European cities to pluvial flooding. *Hydrol Earth Syst Sci* 21: 4131–4147. https://doi.org/10.5194/hess-21-4131-2017
34. Seybatou DIEYE, Mapathé NDIAYE, Diogoye DIOUF, et al. (2024) Flood risk modelling using the hierarchical process analysis (HPA) method: Example of the city of Thies, Senegal. *World J Adv Res Rev* 24: 2440–2657. https://doi.org/10.30574/wjarr.2024.24.3.3989
35. Kangana N, Kankanamge N, De Silva C, et al. (2025) Harnessing mobile technology for flood disaster readiness and response: A comprehensive review of mobile applications on the Google Play Store. *Urban Sci* 9: 106. https://doi.org/10.3390/urbansci9040106
36. Chapi K, Singh VP, Shirzadi A, et al. (2017) A novel hybrid artificial intelligence approach for flood susceptibility assessment. *Environ Model Softw* 95: 229–245. https://doi.org/10.1016/j.envsoft.2017.06.012
37. Band SS, Janizadeh S, Pal SC, et al. (2020) Flash flood susceptibility modeling using new approaches of hybrid and ensemble tree-based machine learning algorithms. *Remote Sens* 12: 3568. https://doi.org/10.3390/rs12213568
38. Khosravi K, Shahabi H, Pham BT, et al. (2019) A comparative assessment of flood susceptibility modeling using multi-criteria decision-making analysis and machine learning methods. *J Hydrol* 573: 311–323. https://doi.org/10.1016/j.jhydrol.2019.03.073
39. Shafizadeh-Moghadam H, Valavi R, Shahabi H, et al. (2018) Novel forecasting approaches using combination of machine learning and statistical models for flood susceptibility mapping. *J Environ Manage* 217: 1–11. https://doi.org/10.1016/j.jenvman.2018.03.089
40. Darabi H, Choubin B, Rahmati O, et al. (2019) Urban flood risk mapping using the GARP and QUEST models: A comparative study of machine learning techniques. *J Hydrol* 569: 142–154. https://doi.org/10.1016/j.jhydrol.2018.12.002
41. Kangana N, Kankanamge N, De Silva C, et al. (2024) Bridging community engagement and technological innovation for creating smart and resilient cities: A systematic literature review. *Smart Cities* 7: 3823–3852. https://doi.org/10.3390/smartcities7060147
42. Dodangeh E, Choubin B, Eigdir AN, et al. (2020) Integrated machine learning methods with resampling algorithms for flood susceptibility prediction. *Sci Total Environ* 705: 135983. https://doi.org/10.1016/j.scitotenv.2019.135983
43. Swain KC, Singha C, Nayak L, (2020) Flood susceptibility mapping through the GIS-AHP technique using the cloud. *ISPRS Int J Geoinf* 9: 720. https://doi.org/10.3390/ijgi9120720
44. Mahmoud SH, Gan TY (2018) Multi-criteria approach to develop flood susceptibility maps in arid regions of Middle East. *J Clean Prod* 196: 216–229. https://doi.org/10.1016/j.jclepro.2018.06.047
45. Das S (2019) Geospatial mapping of flood susceptibility and hydro-geomorphic response to the floods in Ulhas basin, India. *Remote Sens Appl Soc Environ* 14: 60–74. https://doi.org/10.1016/j.rsase.2019.02.006
46. Park K, Lee MH (2019) The development and application of the urban flood risk assessment model for reflecting upon urban planning elements. *Water* 8: 920. https://doi.org/10.3390/w11050920

47. Piyumi MMM, Abenayake C, Jayasinghe A, et al. (2021) Urban flood modeling application: Assess the effectiveness of building regulation in coping with urban flooding under precipitation uncertainty. *Sustain Cities Soc* 75: 103294. https://doi.org/10.1016/j.scs.2021.103294
48. de Silva MMGT, Weerakoon SB, Herath S (2014) Modeling of event and continuous flow hydrographs with HEC–HMS: case study in the Kelani River Basin, Sri Lanka. *J Hydrol Eng* 19: 800–806. https://doi.org/10.1061/(ASCE)HE.1943-5584.0000846
49. Wickramaarachchi TN, Ishidaira H, Wijayaratna TMN (2012) An application of distributed hydrological model, YHyM/BTOPMC to gin ganga watershed, Sri Lanka. *Eng J Inst Eng Sri Lanka* 45: 31–40. https://doi.org/10.4038/engineer.v45i2.7018
50. Dushyantha C, Ptuhina I (2020) Flood risk assessment of river "Kelani Ganga" exceeding its threshold water level. *E3S Web Conf* 157: 02006. https://doi.org/10.1051/e3sconf/202015702006
51. Balica SF, Douben N, Wright NG (2009) Flood vulnerability indices at varying spatial scales. *Water Sci Technol* 60: 2571–2580. https://doi.org/10.2166/wst.2009.183
52. Khosravi K, Pham BT, Chapi K, et al. (2018) A comparative assessment of decision trees algorithms for flash flood susceptibility modeling at Haraz watershed, northern Iran. *Sci Total Environ* 627: 744–755. https://doi.org/10.1016/j.scitotenv.2018.01.266
53. Tehrany MS, Pradhan B, Jebur MN (2014) Flood susceptibility mapping using a novel ensemble weights-of-evidence and support vector machine models in GIS. *J Hydrol* 512: 332–343. https://doi.org/10.1016/j.jhydrol.2014.03.008
54. Meybeck M, Green P, Vörösmarty C (2001) A new typology for mountains and other relief classes. *Mt Res Dev* 21: 34–45. https://doi.org/10.1659/0276-4741(2001)021[0034:ANTFMA]2.0.CO;2
55. Rahmati O, Pourghasemi HR, Zeinivand H (2016) Flood susceptibility mapping using frequency ratio and weights-of-evidence models in the Golastan Province, Iran. *Geocarto Int* 31: 42–70. https://doi.org/10.1080/10106049.2015.1041559
56. Mitra R, Das J (2022) A comparative assessment of flood susceptibility modelling of GIS-based TOPSIS, VIKOR, and EDAS techniques in the Sub-Himalayan foothills region of Eastern India. *Environ Sci Pollut Res* 29: 28999–29013. https://doi.org/10.1007/s11356-022-20839-2
57. Moreira LL, de Brito MM, Kobiyama M (2021) A systematic review and future prospects of flood vulnerability indices. *Nat Hazards Earth Syst Sci* 21: 1–23. https://doi.org/10.5194/nhess-21-1513-2021
58. Liu X, Hu G, Ai B, et al. (2015) A Normalized Urban Areas Composite Index (NUACI) based on combination of DMSP-OLS and MODIS for mapping impervious surface area. *Remote Sens* 7: 17168–17189. https://doi.org/10.3390/rs71215863
59. Tong L, Hu S, Frazier AE (2018) Mixed accuracy of nighttime lights (NTL)-based urban land identification using thresholds: Evidence from a hierarchical analysis in Wuhan Metropolis, China. *Appl Geogr* 98: 201–214. https://doi.org/10.1016/j.apgeog.2018.07.017
60. Ranaweera DKDA, Ratnayake RMK (2016) Urban Landuse Changes in Sri Lanka with Special Reference to Kaduwela Town from 1975 to 2016. *Int J Innov Res Dev* 6: 1–9. https://doi.org/10.24940/ijird/2017/v6/i6/JUN17014

AIMS Press